# Induction Motor IFOC Based Speed-controlled Drive with Asymptotic Disturbance Compensation

## Djordje M. Stojić[1], Milić R. Stojić[2]

**Abstract:** This paper presents the design of digitally controlled speed electrical drive, with the asymptotic compensation of external disturbances, implemented by using the IFOC (Indirect Field Oriented Control) torque controlled induction motor. The asymptotic disturbance compensation is achieved by using the DOB (Disturbance Observer) with the IMP (Internal Model Principle). When compared to the existing IMP-based DOB solutions, in this paper the robust stability and disturbance compensation are improved by implementing the minimal order DOB filter. Also, the IMP-based DOB design is improved by employing the asymptotic compensation of all elemental or more complex external disturbances. The dynamic model of the IFOC torque electrical drive is, also, included in the speed-controller and DOB section design. The simulation and experimental measurements presented in the paper illustrate the effectiveness and robustness of the proposed control scheme.

**Keywords:** Disturbance observer, Asymptotic disturbance compensation, IFOC speed-controlled drive.

## 1   Introduction

One of the goals in the design of feedback control systems is the compensation of external disturbances. To perform this task a number of control structures have been proposed, which can be classified into the following three groups: (i) control schemes based on the IMC (Internal Model Control); (ii) schemes based on the IMP (Internal Model Principle); and (iii) DOB (Disturbance Observer) schemes.

The IMC-based solutions are used in combination with conventional controllers [1] for regulation in different fields of engineering, including motor drive applications. They enable the suppression of external disturbances but, when compared to DOB, are less robust against the effect of unknown external disturbances. When compared to IMC, the IMP-based solutions [2-4] enable the asymptotic compensation of a particular class of external disturbances, yet they

---

[1]Electrical Institute 'Nikola Tesla', University of Belgrade, Koste Glavinica 8a, 11000 Belgrade, Serbia; E-mail: djordje.stojic@ieent.org
[2]School of Electrical Engineering, University of Belgrade, Bulevar Kralja Aleksandra 73, 11000 Belgrade, Serbia; E-mail: estojic@etf.bg.rs

are similarly less robust against the effects of unknown external disturbances when compared to DOB.

To overcome the shortcomings of the IMP and IMC controlling structures, the DOB-based solutions are proposed in [5 – 10] and [13 – 16]. However, the disturbance extraction in [6 – 10] is restricted by the cut-off frequency of the DOB filter. Namely, a decrease of DOB filter cut-off frequency increases the steady-state error caused by the propagation of non-constant external disturbances [5]. Therefore, in [5], the steady-state error caused by external disturbances is reduced by increasing the DOB filter order. However, an increase of DOB filter order prolongs the response time of disturbance observer, and reduces the overall system robustness.

In [5, 13 – 16] several improvements of DOB are proposed. They combine the DOB and IMP, by enabling the asymptotic compensation of a known class of external disturbances, regardless of the DOB filter bandwidth. When compared to the IMP-based DOB solutions, given in the aforementioned papers (based on Gopinath [17] DOB filter design method), the DOB proposed in this paper operates with the smaller filter order, consequently enabling a higher degree of system robustness with respect to model parameter variables. Also, the DOB and controller design procedures, proposed in this paper, include the dynamics of both mechanical and electrical drive subsystems, i.e. besides the drive inertia, the dynamics of the IFOC drive torque response is modelled and included in the DOB filter design procedure. Together with the disturbance compensation, the proportional-differential control law is applied, which includes the original parameter tuning algorithm, proposed in accordance with the plant model transfer function.

The efficiency of the proposed DOB controlling structure is verified by using a speed-controlled electrical drive with an induction motor. The simulation runs and experimental measurements have been performed in the presence of ramp and sinusoidal external disturbances. The drive sensitivity with respect to variations of plant parameters is also examined through experimental tests.

The paper is organized into four sections. In Section 2 the modified DOB control structure, together with the speed-controller, is described in detail. It is shown analytically that the proposed controlling structure enables the desired continuous-time set-point transient response and asymptotic compensation of external torque disturbances to be achieved independently. In Section 3 the simulation results are presented for the ramp and sinusoidal external disturbances. The experimental set-up and measuring results are given in Section 4.

## 2 Speed-controlled Drive with Asymptotic Disturbance Observer

Fig. 1 shows the structure of a digitally-controlled induction motor drive. In the minor loop, the proposed IMP-based DOB is applied. The induction motor drive is based on the IFOC (Indirect Field Oriented Control) torque control algorithm. The nominal plant model $G_P(s) = \omega(s)/T_{ref}(s)$ comprises the IFOC drive model and mechanical inertia model of the motor drive. The control portion of the structure includes the inverse nominal plant model and controller $C(z)$ with proportional-differential control action (PD), while the DOB for the asymptotic disturbance compensation is implemented in the form of filter $Q(z) = N(z)/D(z)$. The output of the control and DOB section $u$ is bounded by the margins that correspond to the saturation effect of the IFOC torque drive. Consequently, by limiting the IFOC drive input $T_{ref}$, the oscillations caused by the torque drive saturation effects are avoided.
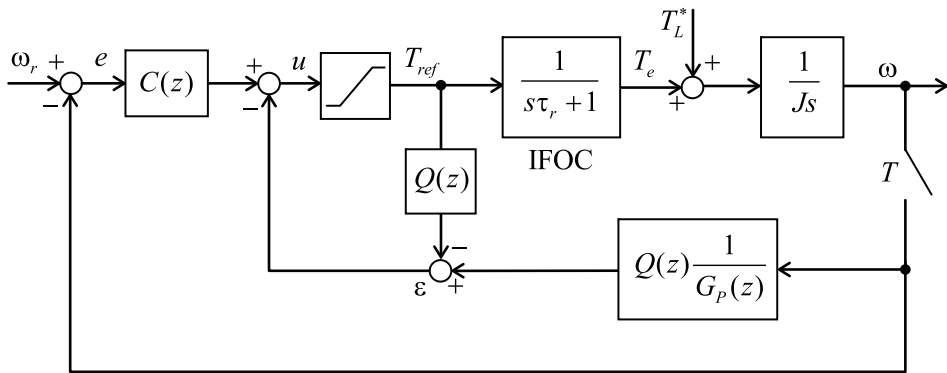


**Fig. 1** – IMP-*based* DOB *speed-controlled drive.*

The discrete zero-order hold equivalent nominal model of the control plant includes: an IFOC based induction motor drive represented by the equivalent first-order transfer function (defined by the dynamics of the IFOC drive torque response, represented by the first order transfer function with the pole characterized by the induction motor rotor time constant $\tau_r = L_r/R_r$ ); and the transfer function of the mechanical drive subsystem dynamics. Hence, the zero-order hold equivalent nominal plant model is approximated by:

$$G_p(z) = \frac{\omega(z)}{T_{ref}(z)} = Z\left[\frac{1}{J(s\tau_r+1)s}\cdot\frac{(1-e^{-Ts})}{s}\right] \tag{1}$$

from which one obtains:

$$G_p(z) = \frac{\omega(z)}{T_{ref}(z)} = C_m\frac{z+\alpha_m}{(z-\beta_m)(z-1)}. \tag{2}$$

The discrete plan model parameters $C_m$, $\alpha_m$ and $\beta_m$ are calculated from IFOC and drive inertia parameter values $J$, $K_{IFOC}$, and $\tau_r$, together with the value of sampling period $T_s$ set to 1 ms.

Notice that the design of the speed-controller and the disturbance observer is based on the nominal plant model. However, the plant model can differ from the nominal owing to variations of model parameters in various drive-operating conditions. For example, the temperature drift represents one of the major causes of the variation of IFOC drive parameters [11]. Therefore, the drive robustness to variations of plant parameters is analysed in the paper by means of simulation, and experimentally in the subsequent sections.

The controlling structure of Fig. 1 comprises the following two parts: the main speed control loop; and the disturbance observer in the minor local loop. The main control loop is designed according to the desired set-point transient response, typical for the speed-servo drives (100 Hz closed-loop control system cut-off frequency), which is achieved by the means of PD (Proportional-differential) controller.

The minor control loop with IMP-based disturbance observer is designed to compensate asymptotically for a known class of external disturbances.

## 2.1. Rejection of disturbance

The difference between the DOB-based disturbance compensation, based on the general purpose filter, and DOB with the asymptotic disturbance compensation is that the second one includes the discrete model of disturbance in the DOB filter design process. Consequently, the asymptotic compensation of the disturbance is implemented, even in the case when the inverse plant model-based disturbance observation is interfered with by the low-pass filter included in the DOB minor loop.

Namely, for the particular class of external disturbances, modelled by the pulse response discrete function $A(z)/B(z)$, the asymptotic disturbance compensation, according to [13], for the DOB control structure given in Fig. 1, is enabled if the following condition is met:

$$\lim_{z \to 1} \frac{z-1}{z} \left[ 1 - \frac{N(z)}{D(z)} \right] \frac{A(z)}{B(z)} = 0 \,, \tag{3}$$

where $Q(z) = N(z)/D(z)$ represents the DOB filter.

Thus, for a stable low-pass digital filter $D(1) \neq 0$ and for any disturbance $A(1) \neq 0$ and $B(1) \neq 0$, the equation (3) is satisfied for:

$$D(z) - N(z) = B(z) \,. \tag{4}$$

Consequently, according to (4), the external load torque disturbance $T_L(z) = A(z)/B(z)$ is rejected asymptotically from the steady-state value of motor speed for

$$N(z) = D(z) - B(z),\qquad(5)$$

where $Q(z) = N(z)/D(z)$ represents the DOB filter transfer function.

Consequently, the design of the DOB filter is based on the discrete disturbance model polynomial $B(z)$ and the filter polynomial $D(z)$, while the resulting numerator polynomial $N(z)$ is derived from (5). In order to obtain the proper DOB filter transfer function $Q(z) = N(z)/D(z)$, it is necessary to employ the filter polynomial $D(z)$, with the order equal to or larger than the order of the disturbance polynomial $B(z)$. Since the basic idea implemented in this paper is to employ the minimal order DOB filter, in order to obtain the robust drive operation against parameter variations, the order of polynomial $D(z)$ is set to be equal to the order of $B(z)$, $n_d = n_b$. Since the leading coefficients of the polynomials $D(z)$ and $B(z)$ are equal to one, the resulting $N(z)$ polynomial (11) has the order $n_n = n_b - 1$. This ensures that $Q(z)/G_p(z)$, present in the local DOB loop given in Fig. 1, can be implemented as a proper transfer function.

The disturbance model polynomials $B(z)$ used in (5) are obtained from their discrete $Z$ transforms. For the step disturbance $B(z) = (z-1)$, the first-order filter polynomial $D(z)$ is employed in (5); for the ramp $B(z) = (z-1)^2$ and sinusoidal $B(z) = (z^2 - 2z\cos\omega T + 1)$ disturbances, the second order polynomial $D(z)$ is used, and so on. Furthermore, the disturbance polynomial $B(z)$ can also be determined in cases of more complex disturbances. For example, for the disturbance composed of the superposed ramp profile and sinusoidal signals, the polynomial $B(z) = (z-1)^2(z^2 - 2z\cos\omega T + 1)$ should be used for the DOB filter design. In this way, for any kind of elemental and combined disturbances, the corresponding polynomial $N(z)$ can be determined by using (5).

It is also necessary to adopt the appropriate filter polynomial $D(z)$, according to the required DOB filter bandwidth, determined by the noise level present in the measurement signal. In this paper, the DOB filter with a bandwidth of 100 Hz, is implemented. Hence, the denominator polynomial of Butterworth's filter [12] with the order equal to the order of $B(z)$ is adopted for $D(z)$. In this way, combined with polynomial $N(z)$ in (5), the DOB filter with the appropriate cut-off frequency is calculated.

In **Table 1**, the numerator $N(z)$ and denominator $D(z)$ of the DOB filter, designed for five different kinds of external disturbances, are presented. The filter polynomials are adopted so as to obtain 100 Hz DOB filter cut-off frequency. The DOB filters are designed for the step, ramp, parabolic and sinusoidal disturbances of 10 Hz and 50 Hz. The DOB compensation and main controller loop operate with the sampling period $T = 1 \text{ms}$.

**Table 1**
*The* DOB *filters designed for bandwidth of* 100 Hz.

| Disturbance | $B(z)$ | $N(z)$ | $D(z)$ |
|---|---|---|---|
| Step | $Z - 1$ | 0.1184 | $z - 0.8816$ |
| Ramp | $(z - 1)^2$ | $0.3525\, z - 0.2991$ | $z^2 - 1.6475\, z +$ <br> $+ 0.7009$ |
| Parabolic | $(z - 1)^3$ | $0.5014\, z^2 - 0.8847\, z +$ <br> $+ 0.3959$ | $z^3 - 2.4986z^2 +$ <br> $+ 2.1153\, z - 0.6041$ |
| Sinusoidal 10 Hz | $z^2 - 1.9961\, z + 1$ | $0.3486\, z - 0.2991$ | $z^2 - 1.6475\, z +$ <br> $+ 0.7009$ |
| Sinusoidal 50 Hz | $z^2 - 1.9021\, z + 1$ | $0.2547\, z - 0.2991$ | $z^2 - 1.6475\, z +$ <br> $+ 0.7009$ |

When compared to the DOB filter proposed in [5] and [16], the filters given in **Table 1** have lower orders, thus enabling the DOB control with increased robust stability. Also, when compared to [13] and [14], the DOB design proposed in this paper enables the asymptotic compensation of all elemental (ramp, parabolic, sinusoidal, etc.) or complex disturbances, which represent the combination of elemental disturbances. Furthermore, in the controlling structure proposed in this paper it is possible to adjust the bandwidth of the DOB to increase the speed of disturbance compensation, and to provide higher system robustness.

## 2.2. Setting of the speed-controller parameter

Controller $C(z)$ of the DOB structure of Fig. 1 can be determined according to the desired poles of the closed-loop system transfer function, derived from the discrete plant transfer function (2)

$$\frac{\omega(z)}{\omega_r(z)} = \frac{G_p(z)C(z)}{1 + G_p(z)C(z)} = \frac{C_m \dfrac{z + \alpha_m}{(z - \beta_m)(z - 1)} C(z)}{1 + C_m \dfrac{z + \alpha_m}{(z - \beta_m)(z - 1)} C(z)} \,. \tag{6}$$

The desired pole placement of the closed-loop transfer function (6) is determined by the required bandwidth of the speed-control drive, equal to 100 Hz. Consequently, in order to achieve this goal, the modified differential control action is adopted for $C(z)$:

$$C(z) = K_p \frac{z - \alpha_d}{z - \beta_d}, \tag{7}$$

where the difference between the common and modified PD action is that, in the former, the $\beta_d = 0$, while in the latter the $\beta_d \neq 0$ value is adopted, in order to reduce the differential ripple and to lower the drive sensitivity in relation to the measurement noise. For $\alpha_d$ in (7), the value equal to the discrete plant model pole $\beta_m$ is adopted, in order to cancel out the influence of the IFOC drive dynamics on the speed-controller performance.

Consequently, the following closed-loop transfer function is obtained:

$$\frac{\omega(z)}{\omega_r(z)} = \frac{C_m \dfrac{z + \alpha_m}{(z - \beta_m)(z - 1)} K_p \dfrac{z - \alpha_d}{z - \beta_d}}{1 + C_m \dfrac{z + \alpha_m}{(z - \beta_m)(z - 1)} K_p \dfrac{z - \alpha_d}{z - \beta_d}} = \frac{C_m K_p (z + \alpha_m)}{(z - 1)(z - \beta_d) + C_m K_p (z + \alpha_m)}, \tag{8}$$

where $\alpha_m$, $\beta_m$ and $C_m$ are attained from the 'zero-hold' discrete equivalent of the plant model transfer function, obtained for the sampling period $T_s = 1\,\text{ms}$.

Therefore, the characteristic polynomial of the closed loop transfer function is equal to

$$P(z) = z^2 + (C_m K_p - 1 - \beta_d)z + \beta_d + C_m K_p \alpha_m. \tag{9}$$

This polynomial is equal to $z^2 - 2\rho\cos(\omega_n T_s)z + \rho^2$, where $\omega_n$ is equivalent to the required bandwidth frequency of the speed control loop, and $\rho$ to the required dumping factor of the speed response. Consequently, the values of $K_p$ and $\beta_d$, which meet the requirement for the set control loop bandwidth and required speed response defined by $\omega_n$ and $\rho$, are obtained by solving the following set of equations:

$$C_m K_p - 1 - \beta_d = -2\cos(\omega_n T_s),$$
$$\beta_d + C_m K_p \alpha_m = \rho^2, \tag{10}$$

resulting in

$$K_p = \frac{[\rho^2 - 2\rho\cos(\omega_n T_s) + 1]}{C_m(1 + \alpha_m)},$$
$$\beta_d = \frac{[\rho^2 + 2\rho\alpha_m\cos(\omega_n T_s) - \alpha_m]}{(1 + \alpha_m)}. \tag{11}$$

Since for the closed-loop system a cut-off frequency of 100 Hz is chosen, with the aperiodic speed response defined by $\rho = 0.7$, for the sampling period

$T = 1\,\text{ms}$, IFOC drive time constant $\tau_r = 0.035\,\text{s}$, and motor inertia $J = 1.6863\,\text{kg m}^2$, the controller parameters $K_p = 18383$, $\beta_d = 0.3123$, and $\alpha_d = \beta_m = 0.9672$ are obtained.

It should be noted that the torque reference signal ($T_{ref}$ in Fig. 1) at the regulator output needs to be limited in accordance with the torque margins, determined by the torque driving characteristics of the IFOC drive. The constrained torque command $T_{ref}$ is fed into the IFOC drive section and the disturbance observer section (see Fig. 1).

## 3    Simulation

In order to examine the efficiency of the proposed DOB in the asymptotic compensation of load torque disturbances, several simulation runs are carried out. Firstly, drive operation in the presence of ramp-profiled external disturbances is analysed. Secondly, the drive operation in the presence of 10 Hz sinusoidal disturbance is examined. Finally, the system robustness, with the respect to uncertainty of the control plant parameters, is analysed.

To illustrate the advantages of the IMP-based DOB design over the DOB based on the general purpose low-pass DOB filter, the corresponding simulation runs for both cases are carried out and compared.
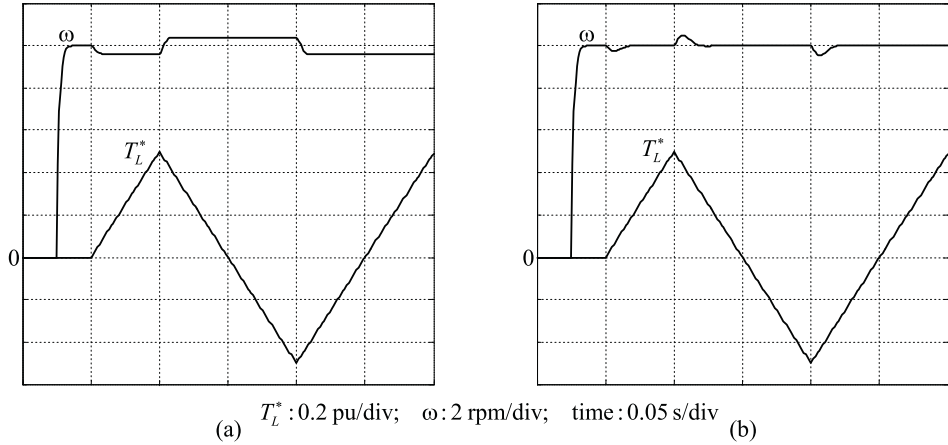
### 3.1  Asymptotic compensation of ramp disturbance

In the first set of simulation runs given in Fig. 2, the system behaviour in the presence of the ramp-profiled torque disturbance is analysed. The disturbance polynomial $B(z) = (z-1)^2$ that corresponds to the extraction of ramp disturbances is applied. The corresponding DOB filter (12) is given in **Table 1** for the DOB filter cut-off frequency 100 Hz, ramp disturbance asymptotic compensation, and sampling period 1 ms.

$$\frac{N(z)}{D(z)} = \frac{0.3525z - 0.2991}{z^2 - 1.6475z + 0.7009}. \tag{12}$$

Figs. 2a and 2b show the motor speed set-point transient responses for the step reference excitation from 0 to 10 rpm, in the presence of the ramp-profiled load torque disturbance: (a) for the general purpose DOB low-pass filter with the cut-off frequency 100 Hz; and (b) for the IMP-based DOB filter (12). In both cases, the desired set-point transient response, determined by the closed-loop system transfer function (8), is achieved, corresponding to the 100 Hz bandwidth. However, the simulation results in Figs. 2a and 2b show that the general purpose DOB low-pass filter fails to reject the ramp-profiled external disturbance; i.e., it operates with a steady-state error. However, the IMP-based

DOB filter (12) eliminates the disturbance entirely from the steady-state value of motor speed. Furthermore, the simulation traces show that the disturbance compensation transient time corresponds to the DOB filter bandwidth, set to 100 Hz.



$T_L^*$ : 0.2 pu/div;   $\omega$ : 2 rpm/div;   time : 0.05 s/div

(a)                                                      (b)

**Fig. 2** – *Compensation of the ramp-profiled disturbance*: (a) *with the general purpose DOB filter*;   (b) *with the* IMP-*based* DOB *filter given in* (12).

### 3.2 Asymptotic compensation of 10 Hz sinusoidal disturbance



$T_L^*$ : 0.2 pu/div;   $\omega$ : 2 rpm/div;   time : 0.05 s/div

(a)                                                      (b)
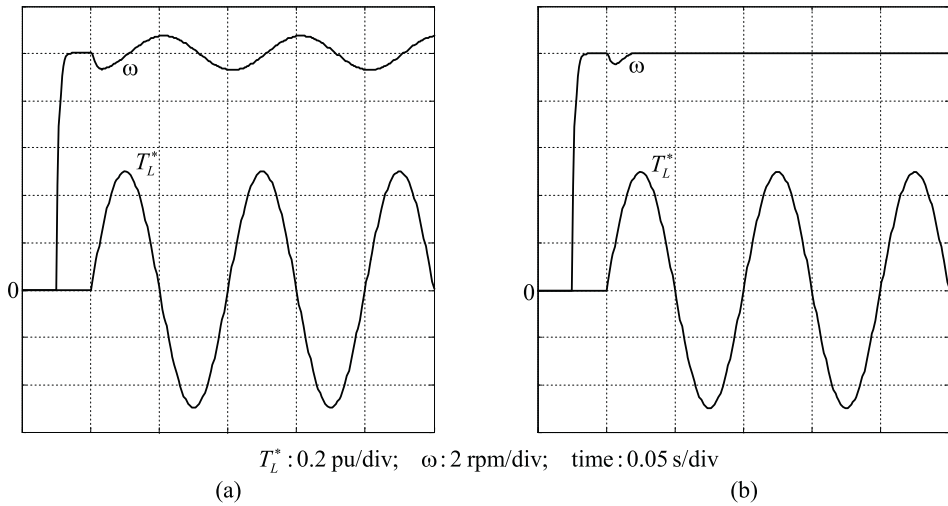
**Fig. 3** – *Compensation of* 10 Hz *sinusoidal disturbance*: (a) *for the general purpose DOB filter*; (b) *for the* IMP-*based* DOB *filter given in* (13).

The second set of simulation runs examines the system performance in the presence of the 10 Hz sinusoidal external disturbance. The simulation results are given in Fig. 3: (a) the traces for general purpose DOB filter; and (b) the traces for the IMP-based DOB filter designed for the asymptotic compensation of the disturbance, given in **Table 1** and in (13)

$$\frac{N(z)}{D(z)} = \frac{0.3486z - 0.2991}{z^2 - 1.6475z + 0.7009} . \tag{13}$$

The simulation results given in Fig. 3 show that the general purpose DOB filter fails to reject the sinusoidal disturbance, while the IMP based DOB filter completely extracts the disturbance from the steady-state value of motor speed. Also, the simulation traces show that the desired transient set-point response corresponding to the closed-loop system bandwidth of 100 Hz is achieved, and that the disturbance compensation response in Fig. 3b is in agreement with the bandwidth of the DOB filter, set to 100 Hz.

### 3.3 System robustness

In this subsection, the robustness of control structure in Fig. 1 is examined against mismatching and/or variations of plant parameters. To this end, the motor inertia $J = 1.6863\,\text{kg m}^2$ is changed to be two times larger than the simulation run given in Fig. 4a, and two times smaller than the simulation run given in Fig. 4b. The robustness is examined in the case of the system with the active sawtooth-profiled external disturbance, with the IMP-based DOB filter (12), designed for the asymptotic compensation of ramp disturbance.
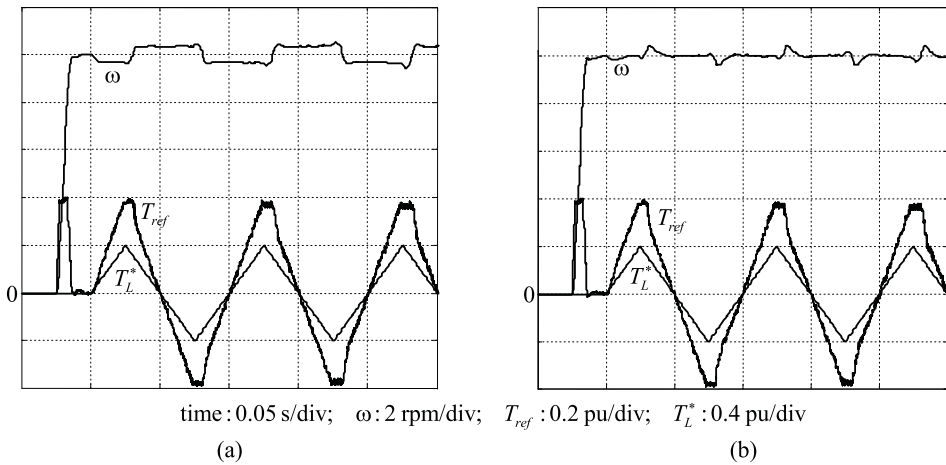


$T_L^* : 0.2\,\text{pu/div}; \quad \omega : 2\,\text{rpm/div}; \quad \text{time} : 0.05\,\text{s/div}$

(a)            (b)
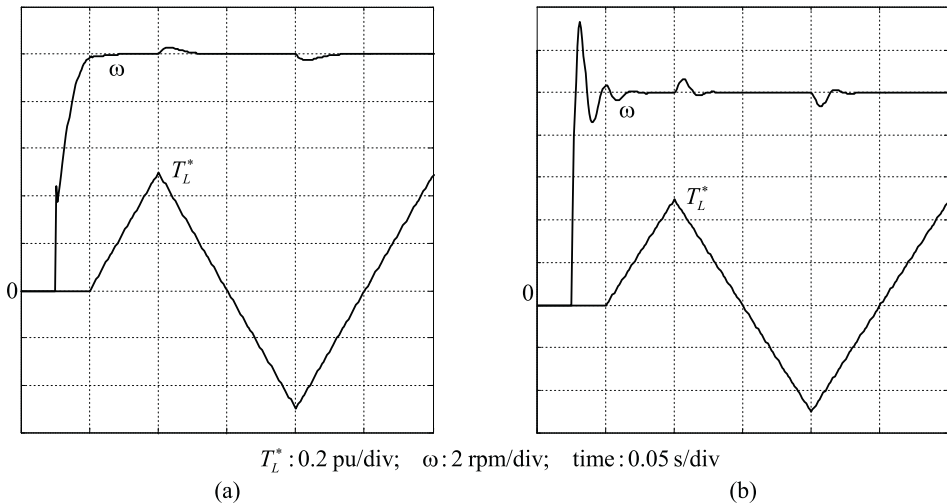
**Fig. 4** – *Compensation of the ramp-profiled disturbance in the case for*:
(a) *two times increased motor inertia J*;  (b) *two times decreased motor inertia J.*

## 4    Experimental Set-up

For experimental verification of the efficiency of the proposed DOB structure in the rejection of external disturbances, the experimental set-up consisted of an IFOC driver 250 W induction motor, coupled with the 500 W DC motor used as the mechanical brake. The nominal induction motor speed is equal to 1500 rpm.

### 4.1  Experimental tests of the DOB with ramp disturbance

In the first set of experimental measurements, the behaviour of the general purpose filter-based DOB and the IMP-based DOB, designed for compensation of the ramp-profiled load torque (12), are examined. The experimental results are presented in Fig. 5, where traces (a) represent the speed response to the reference step excitation from 0 to 10 rpm for the general purpose DOB filter, while traces (b) represent the speed response for the IMP-based DOB filter (12).
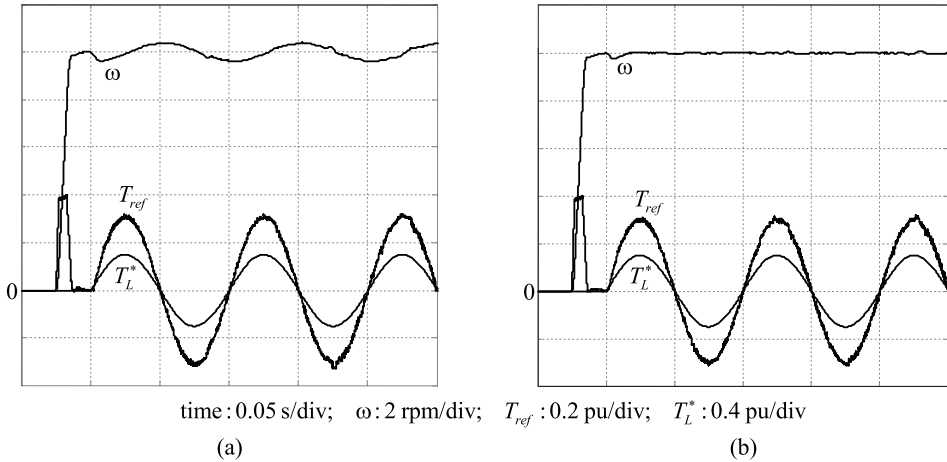


time : 0.05 s/div;    $\omega$ : 2 rpm/div;    $T_{ref}$ : 0.2 pu/div;    $T_L^*$ : 0.4 pu/div

(a)                                                                                  (b)

**Fig. 5** – *Rejection of the ramp-profiled disturbance for*:
(a) *general purpose* DOB *filter*;   (b) *for the* IMP-*based* DOB *filter* (12).

Together with the rotor speed traces, plots in Fig. 5 include traces of the load torque reference $T_L^*$ and torque reference $T_{ref}$, produced by the control algorithm and fed into the IFOC drive, while $T_L^*$ represents the reference for the DC (Direct Current) motor braking armature current, where the $T_{ref}$ is equal to the electromagnetic torque produced by the IFOC-based induction motor drive. In the experimental tests, the step rotor speed reference excitation from 0 to 10 rpm is applied. The traces in Fig. 5 show that the set-point rotor speed transient response corresponds to 100 Hz control loop bandwidth, adjusted by

an appropriate value of controller parameter. Notice that traces in Fig. 5a show that the DOB, based on the general purpose filter, fails to compensate for the sawtooth-profiled load torque; i.e., it operates with a non-zero steady-state value. On the other hand, traces in Fig. 5b show that the IMP-based DOB filter (12) successfully compensates for the sawtooth-profiled load torque, and it operates without steady-state error. The measurement results given in Fig. 5b also show that, during each change of the ramp slope in the sawtooth load torque signal, the disturbance compensation transient period occurs, which corresponds to the DOB filter bandwidth of 100 Hz.

### 4.2 Experimental tests of the DOB with 10 Hz sinusoidal disturbance

In the second set of experiments measurements, the behaviour of the general purpose filter-based DOB and IMP-based DOB, designed for the 10 Hz sinusoidal load torque disturbance compensation (13), is examined. The results of experimental tests are given in Fig. 6. Results in Fig. 6a show that the general purpose DOB filter fails to compensate forthe sinusoidal load torque, while the results of IMP, based on DOB filter (13) in Fig. 6b, show that it enables the drive operation with zero steady-state error. Also, the results in Fig. 6b show that the disturbance compensation transient corresponds to the bandwidth of the DOB filter (16) equal to 100 Hz.
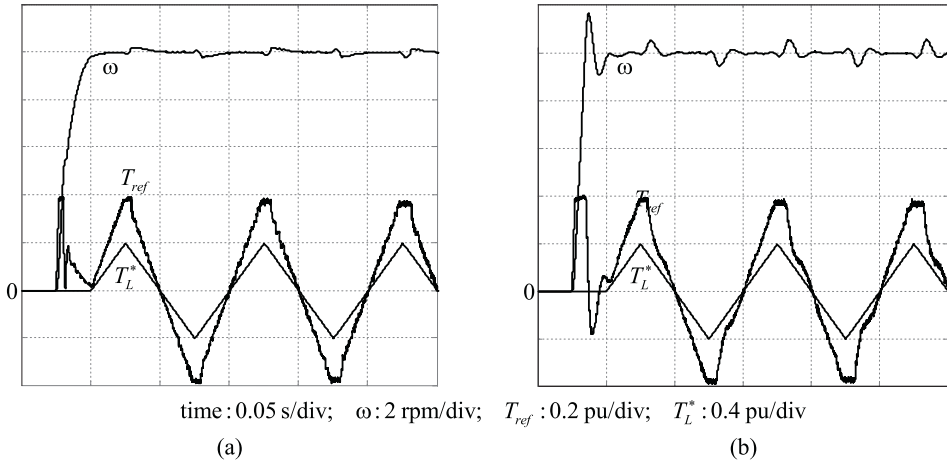


time : 0.05 s/div;   $\omega$ : 2 rpm/div;   $T_{ref}$ : 0.2 pu/div;   $T_L^*$ : 0.4 pu/div

(a)                                                                                              (b)

**Fig. 6** – *Compensation of the* 10 Hz *sinusoidal disturbance for*:
(a) *general purpose* DOB *filter*;   (b) *for the* IMP-*based* DOB *filter* (13).

### 4.3 Experimental test of the proposed DOB robustness

The robustness of the proposed DOB is examined through a series of two experimental tests, in which the equivalent discrete model gain $C_m$ in (2), used for the speed-controller design, is varied over a wide range. In Fig. 7a, traces of the IMP-based DOB filter (12) for the two times decreased $C_m$ value are given

for the ramp-profiled disturbance. In Fig. 7b, the experimental measurements are given for two times the increased Cm value. Both experimental tests show that the significant change in $C_m$ value does not influence the controller stability, while the ramp disturbance rejection is preserved.



time : 0.05 s/div;   $\omega$ : 2 rpm/div;   $T_{ref}$ : 0.2 pu/div;   $T_L^*$ : 0.4 pu/div

(a)                                          (b)

**Fig. 7** – *Rejection of the ramp-profiled disturbance in the case for*:
(a) *two times decreased parameter $C_m$*;   (b) *two times increased parameter $C_m$*.

## 5   Conclusion

The IMP-based DOB design procedure is proposed, which enables asymptotic compensation of a wide class of external disturbances. When compared to the existing IMP-based DOB solutions, the proposed control technique enables the design of the DOB filter of the minimal order, the adjustment of DOB filter bandwidth, and compensation of all elemental or complex disturbances derived from elemental disturbances. While the minimal order of the DOB filter enables the robust operation against the parameter variations, the adjustable DOB filter bandwidth enables the increase of disturbance rejection speed and a reduction of drive sensitivity, in relation to unknown external disturbances. The proposed technique of disturbance compensation is examined analytically, and the resulting DOB filters are tested through a series of simulation runs. The proposed design is also tested by using IFOC-based induction motor speed-controlled drive. The experimental tests for the ramp- and sinusoidal-profiled load torque disturbances are presented, showing that the proposed IMP-based DOB successfully rejects typical classes of external disturbances. The speeds of the system set-point response and disturbance rejection are adjusted analytically by setting values of PD controller parameters and by the desired DOB filter bandwidth. The system robustness of the proposed system is examined by varying the value of the synthetic plant

parameter over a wide range. The simulation and experimental tests show that, for the significant changes of plant parameters, the system preserves the stable operation and ability of disturbance rejection.

# 6  References

[1]   Q. Wang, C. Hang, X. Yang: Single-loop Controller Design via IMC Principles, Automatica, Vol. 37, No. 12, Dec. 2001, pp. 2041 – 2048.

[2]   G. Bengtsson: Output Regulation and Internal Models: A Frequency Domain Approach, Automatica, Vol. 13, No. 4, July 1977, pp. 333 – 345.

[3]   Y. Tsypkin: Stochastic Discrete Systems with Internal Models, Journal of Automation and Information Science, Vol. 29, No. 4-5, 1997, pp. 156 – 161.

[4]   I. Landau, A. Constantinescul, D. Rey: Adaptive Narrowband Disturbance Rejection Applied to an Active Suspension: An Internal Model Principle Approach, Automatica, Vol. 41, No. 4, April 2005, pp. 563 – 574.

[5]   S. Komada, N. Machii, T. Hori: Control of Redundant Manipulators Considering Order of Disturbance Observer, IEEE Transactions on Industrial Electronics, Vol. 47, No.2, April 2000, pp. 413 – 420.

[6]   X. Chen, S. Komada, T. Fukuda: Design of a Nonlinear Disturbance Observer, IEEE Transactions on Industrial Electronics, Vol. 47, No. 2, April 2000, pp. 429 – 437.

[7]   K. Yang, Y. Choi, W. Chung: On the Tracking Performance Improvement of Optical Disk Drive Servo Systems using Error-based Disturbance Observer, IEEE Transactions on Industrial Electronics, Vol. 52, No. 1, Feb. 2005, pp. 270 – 279.

[8]   H. Kobayashi, S. Katsura, K. Ohnishi: An Analysis of Parameter Variations of Disturbance Observer for Motion Control, IEEE Transactions on Industrial Electronics, Vol. 54, No. 6, Dec. 2007, pp. 3413 – 3421.

[9]   S. Katsura, K. Irie, K. Ohishi: Wideband Force Control by Position-acceleration Integrated Disturbance Observer, IEEE Transactions on Industrial Electronics, Vol. 55, No. 4, April 2008, pp. 1699 – 1706.

[10]  C. Kempf, S. Kobayashi: Disturbance Observer and Feedforward Design for a High-speed Direct-drive Positioning Table, IEEE Transactions on Control Systems Technology, Vol. 7, No. 5, Sept. 1999, pp. 513 – 526.

[11]  R. Krishnan, F. Doran: Study of Parameter Sensitivity in High-performance Inverter-fed Induction Motor Drive Systems, IEEE Transaction on Industry Applications, Vol. 23, No. 4, July 1987, pp. 623 – 635.

[12]  A.B. Williams, F.J. Taylors: Electronic Filter Design Handbook, McGraw-Hill, New York, USA, 1988.

[13]  J. Ryoo, K. Jin, J. Moon, M. Chung: Track-following Control using a Disturbance Observer with Asymptotic Disturbance Rejection in High-speed Optical Disk Drives, IEEE Transaction on Consumer Electronics, Vol. 49, No. 4, Nov. 2003, pp. 1178 – 1185.

[14]  Y. Lu: Smooth Speed Control of Motor Drives with Asymptotic Disturbance Compensation, Control Engineering Practice, Vol. 16, No. 5, May 2008, pp. 597 – 608.

[15]  W. Chen: Disturbance Observer based Control for Nonlinear Systems,  IEEE/ASME Transaction on Mechatronics, Vol. 9, No. 4, Dec. 2004, pp. 706 – 710.

[16]  K. Ohnishi, M. Shibata, T. Murakami: Motion Control for Advanced Mechatronics, IEEE/ASME Transactions on Mechatronics, Vol. 1, No. 1, March 1996, pp. 56 – 67.

[17]  B. Gopinath: On the Control of Linear Multiple Input-output Systems, Bell System Technology Journal, Vol. 50, No. 3, March 1971, pp. 1063 – 1081.